*sustainability*

MDPI

*Article*

# Study on Overburden Movement Deformation and Roof Breakage Law of Under-Protective Steeply Inclined Coal Seam Mining

**Xinshan Peng [1], Lingling Qi [1,2,3,4,*], Zhaofeng Wang [1,2,3,4,*], Xiaoqing Zhou [1] and Chunlei Hua [1]**

[1] School of Safety Science and Engineering, Henan Polytechnic University, Jiaozuo 454000, China
[2] MOE Engineering Research Center of Coal Mine Disaster Prevention and Emergency Rescue, Jiaozuo 454000, China
[3] Collaborative Innovation Center of Coal Work Safety and Clean High Efficiency Utilization, Jiaozuo 454000, China
[4] State Key Laboratory Cultivation Base for Gas Geology and Gas Control, Jiaozuo 454000, China
* Correspondence: qll5407@163.com (L.Q.); wzf3988@163.com (Z.W.)

**Abstract:** The occurrence of a steeply inclined coal seam is extraordinary, and the coal body is seriously damaged by extrusion. The most steeply inclined coal seam is a high-gas or -outburst coal seam, and protective layer mining is the safest and most effective measure for regional prevention of coal and gas outburst. Based on considering the coefficient of lateral pressure and vertical height of the section, the deflection of the basic roof of the steeply inclined protective layer in a mine in western Henan, China, was calculated using the deflection calculation method of the thin-plate theory of elasticity. Using MATLAB to understand the deflection, the deflection curve was obtained. The law of rock movement and deformation in the mining process of the protective layer was studied by a similarity simulation experiment. The results show that, after mining, the roof mainly sinks slowly without large-scale collapse, and the largest rock strata movement is located in the upper part of the slope. Rock strata movement and fracture development can relieve the pressure of the protected layer and provide a channel for gas migration and drainage. The mining conditions of the protected layer will not be destroyed, and mining this type of protected layer in this mine has better safety and feasibility. The conclusions of this study have a guiding and scientific significance for the control of surrounding rock and the layout of gas drainage boreholes of under-protective steeply inclined coal seam mining.

**Keywords:** steeply inclined coal seam; protective layer; overburden movement; roof breakage



**Citation:** Peng, X.; Qi, L.; Wang, Z.; Zhou, X.; Hua, C. Study on Overburden Movement Deformation and Roof Breakage Law of Under-Protective Steeply Inclined Coal Seam Mining. *Sustainability* **2022**, *14*, 10068. https://doi.org/10.3390/su141610068

Academic Editors: Jianhang Chen, Danqi Li, Ping Chang and Saisai Wu

Received: 23 July 2022
Accepted: 12 August 2022
Published: 14 August 2022



## 1. Introduction

Coal seams with an occurrence angle of more than 45° are called steeply inclined coal seams, which are recognized as difficult to mine in the mining industry, and a considerable part of them are coal and gas outburst seams. Protective layer mining is considered to be the most effective method to prevent and control coal and gas outburst [1–3]. In 1933, France began to conduct experimental research on protective layer mining, whereafter Germany, Poland, and other countries also began applying this technology to prevent coal and gas outburst [4,5]. Since the late 1950s, China has applied protective layer technology to prevent coal and gas outburst in southwest China and achieved remarkable results [6,7]. Since 1998, Huainan Mining Group has conducted experimental research on exploiting protective layers under various geological conditions and achieved remarkable application effects. The gas control concept of "all that can be protected" has been formed in the Huainan mining area, which has been popularized and applied to high-gas-outburst mining areas in China [8,9]. With the protective layer mining, the stress of the surrounding rock of the stope can be redistributed, and the overlying rock and coal mass of the stope has a pressure

relief area. In a certain period, the stress of the roof of the goaf will be reduced within a specific range, resulting in the expansion and deformation of the coal stratum, which makes the coal stratum move toward the goaf; the unloading and swelling deformation of overlying coal and rock mass can be reflected by the displacement and deformation of roof coal and rock strata to a certain extent [10,11]. Previous studies have shown that with a larger inclination angle of the coal seam, the tangential slip component along the rock layer increases, and the vertical pressure acting on the layer decreases so that the roof subsidence will gradually decrease [12,13]. When mining steeply inclined coal seams, the gangue falling in the goaf cannot stay in place in most cases due to its weight but slides down along the coal seam [14]. The condition of sliding is $tg\alpha > f''$($\alpha$ is the inclined angle of the coal seam, and $f$ is the dynamic friction coefficient of the caving gangue along the coal seam floor). If $f' = 0.6$~$0.7$, when $\alpha > 31$~$35^\circ$, the falling gangue will slip, and the larger the $\alpha$, the larger the sliding, and the more intense it will occur [15–18]. The condition of falling gangue does not simply depend on the inclined angle of the rock stratum but is related to the nature of the roof rock stratum, mining height, and rock stratum thickness [19]. At the initial stage of roof caving, due to the small amount of caving gangue, it is not enough to fill the goaf, and therefore, the interior or upper part of the goaf is in a suspended state [20]. In this case, the section with a suspended roof will produce caving. It may gradually develop upward until the coal pillar above the ventilation roadway so that the gangue stored in the upper old goaf will also slide downward and fill the goaf of this working face. After the goaf is filled, when the working face continues to advance and cave, the rock movement characteristics in different parts of the goaf are different [21–23].

Based on the thin-plate theory of elasticity, this paper focuses on analyzing the law of roof movement and deformation in mining the steep protective layer. On this basis, through a similar simulation test, the movement and deformation law of the protective layer mining under the steep incline and close distance in a mine in western Henan is studied. Then, it is analyzed whether mining this kind of protective layer destroys the mining conditions of the overlying protective layer and whether its safety and feasibility are guaranteed.

## 2. Roof Breaking Regular of Under-Protective Steeply Inclined Coal Seam Mining

### *2.1. Stress Analysis of Steep Roof*

In elasticity, a plate is defined as an object surrounded by two parallel planes and a cylindrical or prismatic surface perpendicular to the two parallel planes [24], as shown in Figure 1. Its geometric feature is that the thickness is much smaller than the dimensions in the other two directions. The nature and calculation method of the plate largely depend on t, the thickness of the plate, and the dimensions in the other two directions [25]; the classification of the plate is shown in Table 1.

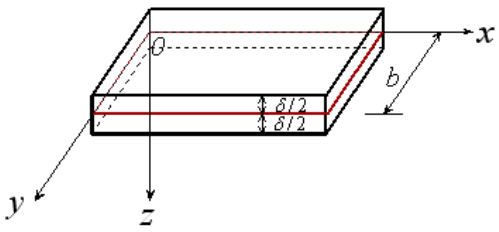


**Figure 1.** The geometric features and coordinates of the board.

**Table 1.** Classification of the board.

| The Type of Plate | The Thin Films | The Thin Plate | The Thick Plate |
|---|---|---|---|
| The ratio of thickness ($\delta$) to minimum side length ($b$) | $\frac{\delta}{b} < (\frac{1}{100} \sim \frac{1}{80})$ | $(\frac{1}{100} \sim \frac{1}{80}) \leq \frac{\delta}{b} \leq (\frac{1}{8} \sim \frac{1}{5})$ | $\frac{\delta}{b} > (\frac{1}{8} \sim \frac{1}{5})$ |

For rock material, its most prominent characteristic is that the compressive strength is greater than the shear strength, and the shear strength is much greater than the tensile strength. Therefore, the uniaxial tensile strength of rock determines its strength, and the main factor affecting the failure of rock mass is the maximum tensile stress [26,27]. Hard rock with greater brittleness has this characteristic, and therefore, the geometric condition of defining a rock plate as a thin plate can be appropriately relaxed [28]. In fact, the coal measure strata are sedimentary strata, the thickness of thick and hard strata in the overlying strata of the stope is limited, usually no more than 20 m, while the size of the goaf is relatively infinite in large-scale mining. In his study of rock slabs, academician Galerkin of the former Soviet Union believed that when $\delta/b \leq 1/5$, the thin-plate method is ultimately allowed. The research of Borisov and others in the former Soviet Union shows that when $\delta/b \leq 1/3$, the thin-plate theory method can also be used [14,29].

In the steeply inclined working face, the rock stratum angle is larger (greater than 45°), and unlike the near-horizontal coal seam, the component action along the rock stratum layer (the inclined direction) cannot be ignored. The component of the force (the inclined direction) along the roof layer of the overlying rock stratum is greater than the normal component along the layer. The roof deformation occurs under the combined action of transverse load and longitudinal load [30,31]. As a brittle material, rock has little tensile strength. The basic roof is prone to fracture under the combined action of transverse load and longitudinal load, and the fracture is a tensile fracture dominated by buckling and instability [32].

According to the No.1-8 coal seam mining in the protective layer of a mine in western Henan, China, its basic roof fully conforms to the geometric conditions of an elastic thin plate. In addition, its deflection must not be greater than the mining thickness of the coal seam, which is also in line with the premise of the thin-plate bending small deflection theory [33]. Based on the above conditions, the basic roof suspended in the upper part of the goaf before the initial pressure can be regarded as an elastic thin plate. A rectangular coordinate system as shown in Figure 2 is established for the convenience of analysis. In the figure, the mining direction along the strike is set as the $x$ axis, and the mining direction along the tilt direction is set as the $y$ axis.

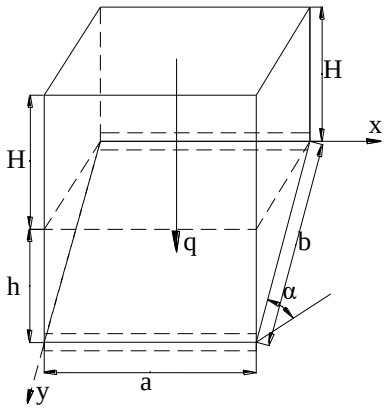


**Figure 2.** Stress analysis of the face roof.

In Figure 2, $a$ is the roof strike fracture length, 60 m; $b$ is the inclined length of the working face, 75 m; $H$ is the buried depth of the air return roadway, 330 m; $h$ is the section vertical height, 57.5 m; and $q$ is the load of the overlying strata, in trapezoidal distribution, MPa.

### *2.2. Analysis of the First Roof Collapse with the Thin-Plate Theory*

Before the basic roof is broken, the basic roof and its overlying strata are supported by the surrounding coal walls. The basic roof is clamped by the coal wall and the overlying strata of the basic roof, and the coal wall and the overlying strata of the basic roof are

overall layered structures in an extensive range [34]. Due to its limitations, in advancing the working face, the four sides of the basic roof can neither rotate nor sink, and only the elastic deformation of the suspended plate in the goaf can occur. This existing feature of the basic roof is consistent with the thin plate with four fixed edges in the thin-plate theory of elasticity. Therefore, the basic top before the initial fracture can be regarded as a thin plate fixed on four sides [35,36], and the calculation model is shown in Figure 3.

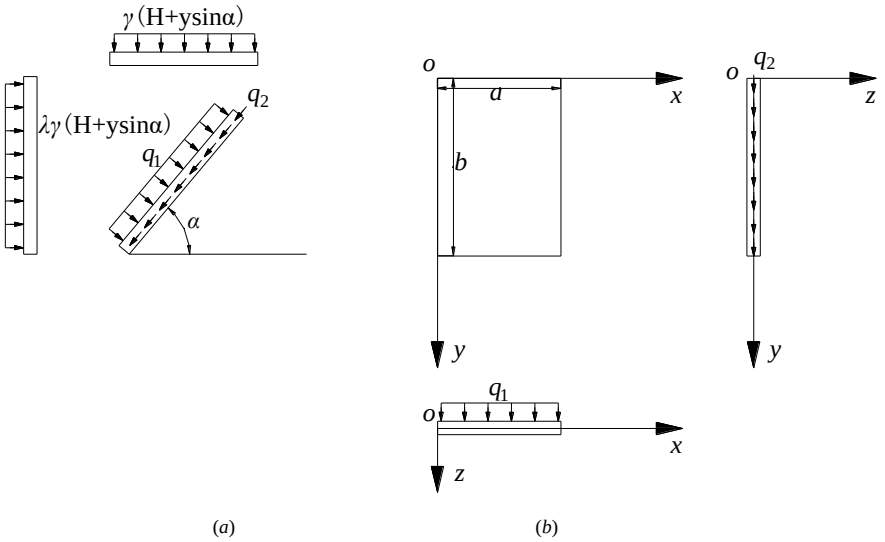


**Figure 3.** The calculation model of the roof initial breaking down. (**a**) The side view. (**b**) The top view.

In Figure 3, $\gamma$ is the unit weight of overburden, 25.6 kN/m$^3$; $\lambda$ is the side pressure coefficient, $\lambda = \frac{\mu'}{1-\mu'}$, with $\mu'$ as Poisson's ratio, taken as 0.24, and the calculated $\lambda$ is 0.316; $\alpha$ is the coal seam inclination, 50°.

The load of the air return roadway at the upper end of the working face is $\gamma H$, and the load of the transportation roadway at the lower end is $\gamma(H+h)$. In the stage of shallow mining depth, the load borne by the slab cannot be calculated according to the uniformly distributed load, and the change in vertical stress along the inclined direction should be considered. Therefore, the action load of the overlying strata can be expressed as $q = \gamma(H + y\sin\alpha)$ [37,38].

Then, the transverse load component can be expressed as Formula (1):

$$q_1 = q(\cos\alpha + \lambda\sin\alpha) = \gamma(H + y\sin\alpha)(\cos\alpha + \lambda\sin\alpha) \quad (1)$$

The longitudinal load component can be expressed as Formula (2):

$$q_2 = q(\sin\alpha - \lambda\cos\alpha) = \gamma(H + y\sin\alpha)(\sin\alpha - \lambda\cos\alpha) \quad (2)$$

From the expressions of transverse and longitudinal load components, it can be seen that the magnitude of the load is related to the lateral pressure coefficient. When there is structural stress, or when the rock stratum enters the large mining depth and is in the hydrostatic pressure stage, the transverse load acting on the slab may be greater than $\gamma(H + y\sin\alpha)$.

The boundary conditions of the model are as follows:

$$(\omega)_{x=0,a} = 0; \qquad (\omega)_{y=0,b} = 0; \qquad \left(\frac{\partial\omega}{\partial x}\right)_{x=0,a} = 0; \qquad \left(\frac{\partial\omega}{\partial y}\right)_{y=0,b} = 0$$

where $\omega(x, y)$ is the assumed roof deflection function.

Choose the Liz method to solve [39], taking a $\omega = c_1\omega_1$ which can meet the needs of mining production.

$$\omega_1 = (1 - \cos\frac{2\pi x}{a})(1 - \cos\frac{2\pi y}{b}) \tag{3}$$

The deformation potential energy of the plate can be expressed as Formula (4):

$$U = \frac{D}{2}\int\int_A \left\{(\nabla^2\omega)^2 - 2(1-\mu)[\frac{\partial^2\omega}{\partial x^2}\frac{\partial^2\omega}{\partial y^2} - (\frac{\partial^2\omega}{\partial x\partial y})^2]\right\}dxdy \tag{4}$$

where $D$ is the bending stiffness of the plate, and $D = \frac{Eh^3}{12(1-\mu'^2)}$; $E$ is the elastic modulus of the roof rock stratum, $1.36 \times 10^4$ MPa; $\mu'$ is Poisson's ratio, taken as 0.24; $h$ is the thickness of the main roof strata participating in the incoming pressure, 4 m; $A$ is the roof exposed area, $A = a \times b$, $m^2$.

The work done by external force can be expressed as Formula (5):

$$W = \iint q_1\omega dxdy + \frac{1}{2}\iint q_2(\frac{\partial\omega}{\partial y})^2 dxdy \tag{5}$$

According to the principle of potential energy,

$$C_1 = \frac{2q_1 b}{8D\pi^4 b(3/a^4 + 3/b^4 + 2/a^2b^2) - 3\pi^2 q_2} \tag{6}$$

The roof deflection equation can be expressed as Formula (7):

$$\omega = \frac{2q_1 b}{8D\pi^4 b(3/a^4 + 3/b^4 + 2/a^2b^2) - 3\pi^2 q_2}(1 - \cos\frac{2\pi x}{a})(1 - \cos\frac{2\pi y}{b}) \tag{7}$$

When the buried depth is shallow, the vertical height difference between the upper and lower roadway is not much less than the average buried depth of the working face. When considering the change of in-situ stress according to the depth of the inclined direction, the maximum deflection point should be located at a point below the middle. In the initial mining stage, before the first roof collapse, there is no filling effect of collapse gangue, and the roof is in the elastic deformation stage. Use MATLAB to calculate and solve the deflection, and the deflection curve is shown in Figure 4. The deflection deformation is symmetrically distributed in the strike. The maximum deflection point in the tendency direction is located slightly below the middle, about 39 m away from the upper end; the maximum deformation is about 270 mm.

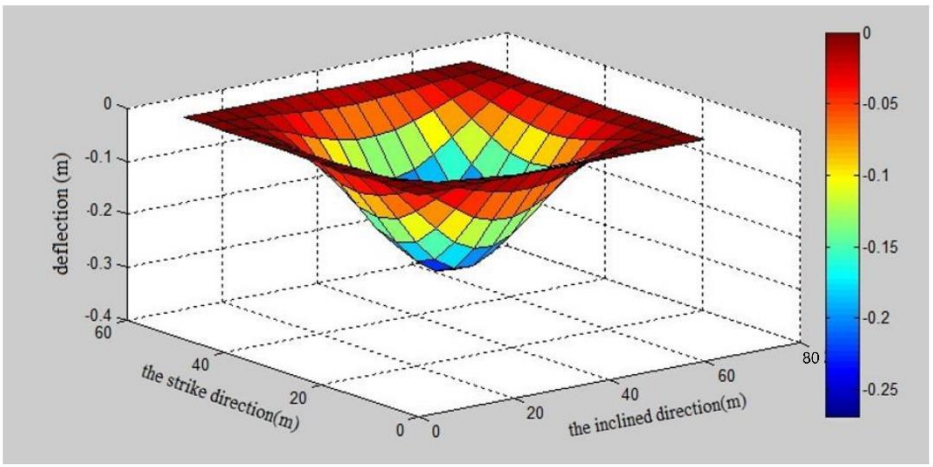


**Figure 4.** The deflection curve in initial roof caving.

### *2.3. Analysis in Normal Mining Stage with the Thin-Plate Theory*

After the first roof collapse, the working face is in the normal mining stage. Due to the filling of the lower part of the goaf by the roof falling gangue, the movement characteristics of the rock blocks under the roof, in the middle, and in the upper part are different [40]. Furthermore, the stacking height and stiffness of the caving gangue have a particular impact on the fracture morphology of the rock block. The model is shown in Figure 5. The roof caving height can convert the $L_k$ of gangue filling, and the effect of the gangue filling foundation can be considered the elastic foundation.

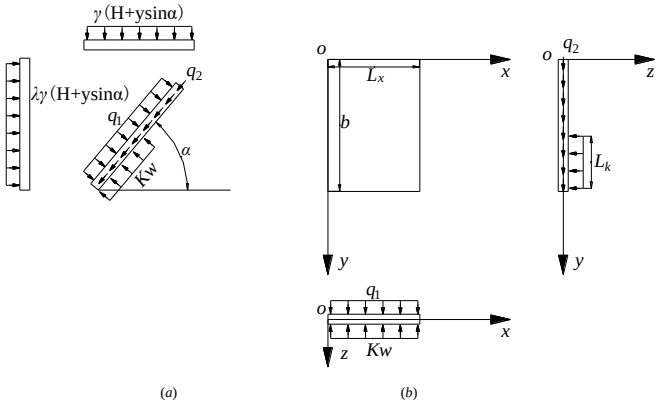


**Figure 5.** Calculation model of the roof caving in normal mining phase. (**a**) The side view. (**b**) The top view.

The research shows that the gangue backfill also has four stages: elastic deformation, yield, plastic deformation, and plastic failure under pressure. Along the width direction of the backfill, the stress distribution is not uniform [41]. If the deflection of the plate is slight (thin-plate small deflection theory) [42], the Winkler–Zimmer hypothesis can be adopted; that is, the reaction force per unit area on the elastic foundation is proportional to the deflection at this point. Therefore, the load borne by the caving and filling gangue can be expressed as Formula (8):

$$F = K\omega \tag{8}$$

In Formula (8), $F$ is the force provided by gangue, MPa; $K$ is the equivalent elastic coefficient of gangue, MPa/m, where the coefficient is 30 MPa/m [43]; $\omega$ is the deflection of the overlying basic roof, m.

Similarly, according to the Ritz method, considering the energy absorbed by the deformation of the gangue elastic foundation, the roof deflection equation in the normal mining stage can be deduced as Formula (9):

$$\omega = \left\{ \frac{3q_1 L_x - \frac{a}{b}(L_k - \frac{b}{2\pi}\sin\frac{2\pi L_k}{b})}{\frac{12D}{b^3}[3L_x^4 - \frac{4\pi^2}{3}L_x^2 - 12(1-\mu')\pi^2 L_x^2 - \frac{8\pi^2}{5}]} \right\} \cdot (\frac{x}{L_k})^2 (1 - \cos\frac{2\pi y}{b}) \tag{9}$$

where $L_x$ is the exposed length of the roof along the strike, 25 m; $L_k$ is the gangue filling length, $L_k = \frac{b}{L_x}$, 3 m.

Formula (9) shows that the main function of gangue filling is to limit the deflection deformation of the roof and increase the pressure step. Similarly, MATLAB is used to calculate and solve the deflection, and the deflection curve is shown in Figure 6. Under the same boundary conditions, the maximum deflection point has an upward trend with the increase in filling height and compactness. The maximum deflection point along the working face inclination is located slightly above the middle, about 34 m away from the upper end, about 5 m higher than the maximum deflection point of the first pressure, and the maximum deformation is about 210 mm, which is less than the maximum deflection of the first collapse.

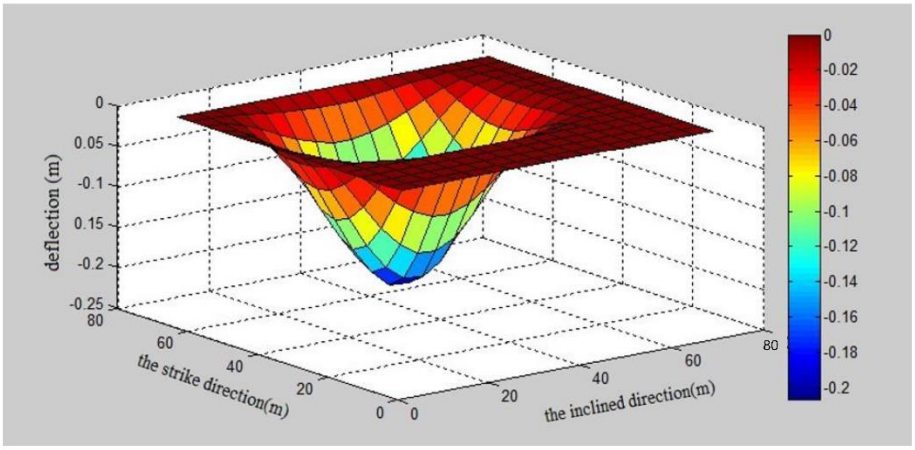


**Figure 6.** The deflection curve in normal mining phase.

## 3. Similar Simulation Experiment of Overburden Movement Deformation of Under-Protective Steeply Inclined Coal Seam Mining

### *3.1. Experimental Model Design*

According to the existing test conditions, it was decided to conduct the test on a rigid model frame with a size of 1.3 m × 0.1 m × 1.1 m (length × width × height) for a similar simulation of the inclined cross-section. The stress was loaded in the vertical direction, and the passive plane constraint was used in the horizontal direction to limit the deformation. According to the test bench, the similarity ratio was determined to be 1:50, the thickness of the simulated coal layer in the vertical direction was 55 m, and the horizontal length was 65 m. The model laying is shown in Figure 7.

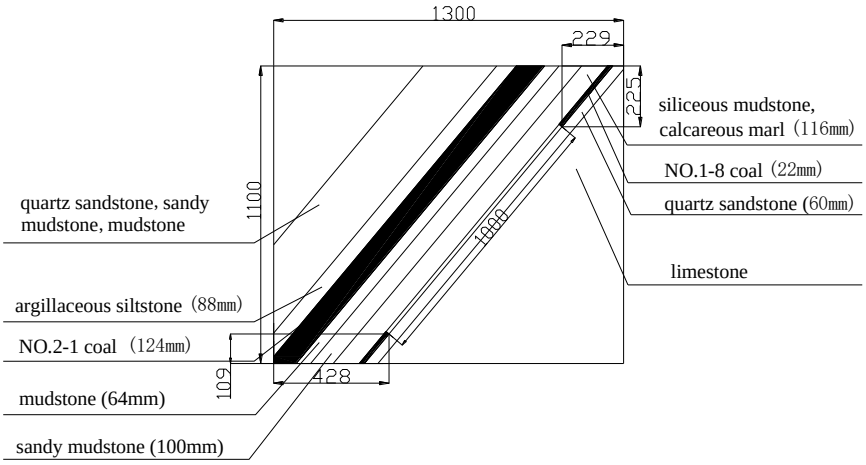


**Figure 7.** The sketch of similar simulation experiment.

### *3.2. Experimental Procedure*

(1) Lay the model

The model was laid according to the material ratio plan and laid from the bottom to the top according to the age of the geological deposition of the rock layer.

(2) Layout of rock stratum mobile measuring points

The steel plate was removed after the model was laid in 3 days, and plaster was painted on the surface of the model after 7 days of drying; artificial signs were attached to the surface of the model, and a displacement gauge was installed on the back of the model. Several displacement-measuring lines were arranged on the roof of No. 1-8 coal and the roof and bottom of No. 2-1 coal. The displacement measuring points were marked with circular diagonal artificial signs supporting the experimental system and were analyzed by

image comparison. The displacement measurement also uses the YHD—30 displacement gauge for comparative and supplementary measurement. The displacement gauge was arranged on the back of the model. The YHD—30 displacement gauge data acquisition system was also a YE2539A high-speed static strain gauge. The model is shown in Figure 8.

(**a**) (**b**)

**Figure 8.** The panorama of modeling experiment. (**a**) The front side of the model. (**b**) The back of the model.

(3) Compensate stress

The upper boundary of the experimental model was buried at a depth of 330 m, and the stress value of the overlying rock layer was calculated according to the bulk density of 8.25 MPa; the bulk density ratio was 0.60, and the stress similarity ratio was 0.012, and therefore, the vertical compensation stress was 0.10 MPa. After the model was dried, the stress was loaded vertically, uniformly, and slowly to 0.10 MPa and loaded for 24 h.

(4) Excavation and data collection

The excavation roadway records data and collects images to record the movement of the overlying strata during the excavation of the protective layer working face.

### *3.3. Experimental Results*

The deformation and movement of the coal and rock mass were caused by the mining action of the lower protective layer, and the overlying coal and rock mass was continuously monitored during the entire protective layer mining process. By comparing the coordinates of each measuring point before and after mining, the movement process and subsidence amount of the coal and rock mass on the protective layer were obtained, as shown in Figure 9.

I—The experimental figure

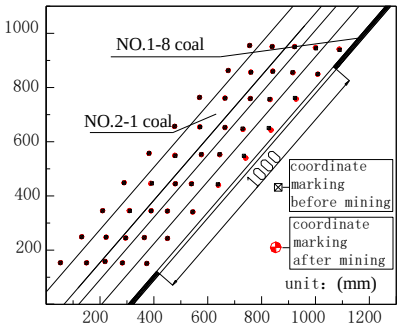


II—Coordinate comparison diagram of measuring points

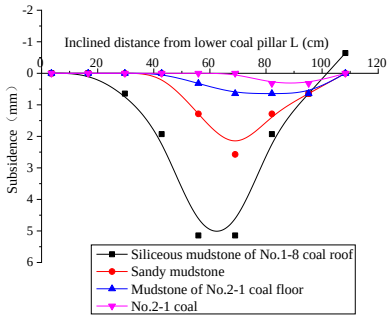


III—Displacement of coal and rock

(**a**)

I—The experimental figure

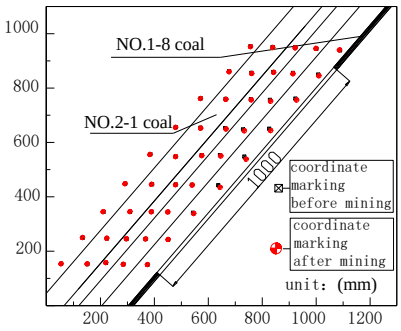


II—Coordinate comparison diagram of measuring points

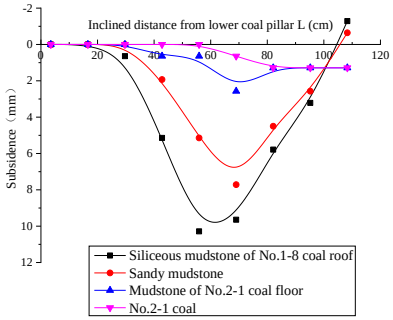


III—Displacement of coal and rock

(**b**)

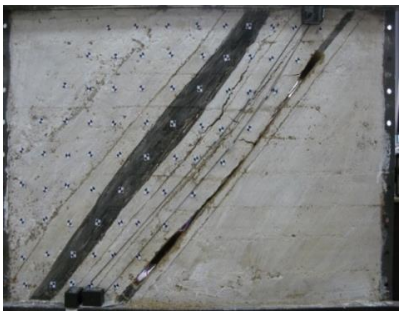

I—The experimental figure

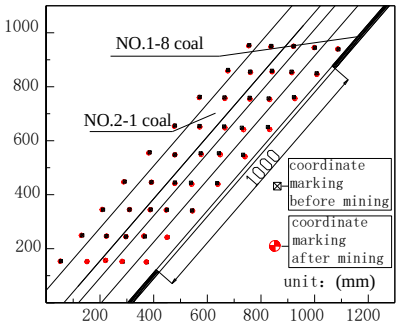


II—Coordinate comparison diagram of measuring points

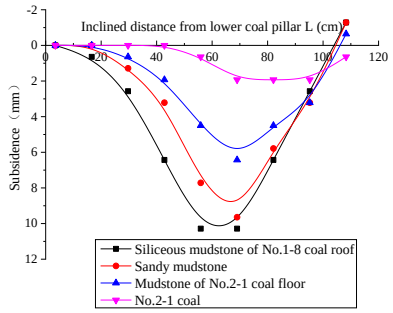


III—Displacement of coal and rock

(**c**)

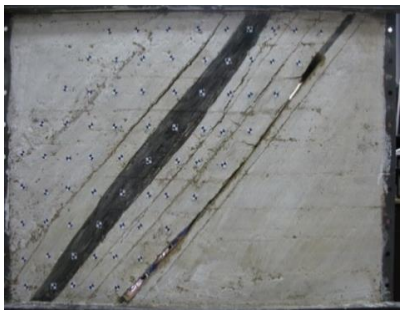

I—The experimental figure

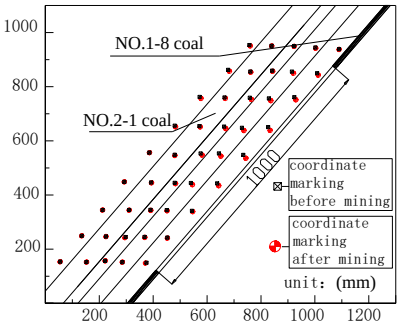


II—Coordinate comparison diagram of measuring points

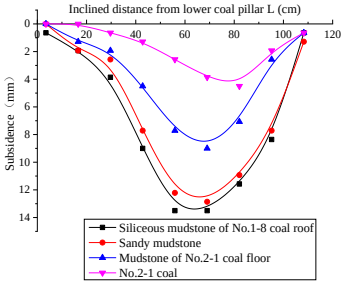


III—Displacement of coal and rock

(**d**)

**Figure 9.** The comparison chart of strata movement. (**a**) The first collapse. (**b**) The second collapse. (**c**) The third collapse. (**d**) End of the mining.

In Figure 9, under the influence of the mining, the overlying coal and rock masses have different degrees of movement and deformation:

(1) When the No. 1-8 coal roof fractures for the first time, the overlying sandy mudstone appears to crack through layers, the cracks at the upper end of the incision hole are abnormally developed, and the roof at the lower end of the tilt develops cracks. The siliceous mudstone on the No. 1-8 coal roof subsides first, with maximum subsidence of about 5 mm, which appears at a position 55 cm away from the lower coal pillar. The overlying sandy mudstone subsides about 3 mm, the mudstone subsides about 1 mm, and the protected layer is not affected by mining.

(2) When the overlying sandy mudstone collapses, the subsidence of each rock layer is intensified, the bedding fractures further extend to the upper and lower ends of the inclined direction, and the interlayer fractures gradually develop from bottom to top along the vertical direction of the rock layer. The maximum subsidence of siliceous mudstone on the roof of No. 1-8 coal is about 10 mm, the subsidence of sandy mudstone is about 8 mm, the subsidence of mudstone is about 3 mm, and No. 2-1 coal also appears at 1~2 mm subsidence.

(3) With the expansion of the mining range, the mudstone of the No. 2-1 coal floor collapses, and the collapsed rock layer squeezes the underlying rock layer, so that the subsidence of the two underlying rock formations also increases, and the No. 2-1 coal also bends and sinks after losing the support of the bottom plate. The siliceous mudstone of the No. 1-8 roof subsides more than 11 mm, and the maximum subsidence of sandy mudstone is slightly less than 10 mm. The maximum subsidence of mudstone exceeds 6 mm, and the maximum subsidence of the No. 2-1 coal also reaches 2 mm.

(4) After mining, the subsidence amount of each coal rock layer reaches the maximum value. At this time, the top floor of No. 1-8 coal is entirely in contact with the bottom plate, and the maximum subsidence is slightly less than 14 mm, almost equal to the thickness of No. 1-8 coal. The maximum subsidence of sandy mudstone is 13 mm, and the amount of separation between siliceous mudstone and sandy mudstone is smaller than before. The maximum subsidence amount of mudstone is about 9 mm, and the subsidence amount of No. 2-1 coal is nearly 6 mm. The floor of No. 2-1 coal has a layer-penetrating fissure, and the roof develops a layer-separating fissure.

(5) During the entire excavation process, there is no large-scale collapse, and the primary method is slow subsidence. The roof collapses for the first time after the working face is more than half excavated. After the roof collapses, it does not slide down the inclination directly but forms a hinged structure in the inclination direction, unlike the structure in which the small-angle coal seam forms an arch.

## 4. Analysis and Discussion

(1) The asymmetry in the inclination of the initial roof collapse is mainly due to the large inclined angle of the steeply sloping coal seam and the uneven load, especially when considering the section vertical height and lateral pressure coefficient. In the working face's initial mining stage, the roof rock is damaged, and the caving is in a relatively violent and unstable state. Therefore, roof collapse accidents are prone to occur on the upper part of the working face and when the new working face is just mined, and roof management should be strengthened according to these characteristics.

(2) In the normal mining stage, although the gangue filling has a supporting effect, the deflection of the roof is still distributed symmetrically along the strike, and the maximum deflection point is in the middle of the overhang boundary strike. The maximum deflection position shifts upward along the slope, which is smaller than the maximum deflection during the initial caving, which is precisely due to the filling effect of the caving gangue.

(3) The deflection of the inclined sheet is proportional to the lateral load and inversely proportional to its bending stiffness. Although the lateral load decreases with the increase in the inclination angle of the rock formation, the existence of the longitudinal load at this time will increase the deflection of the roof, which is also the reason why the roof deformation

degree of steeply inclined coal seams is different from that of near-horizontal and gently inclined coal seams. Due to the complexity of rock mass properties and strata structure in coal mines, the quantitative calculation of thin plates can only provide a qualitative reference for the law of deformation and collapse of the overlying strata.

(4) It can be seen from the fracture and caving characteristics of the roof during the experiment that the maximum subsidence point of each rock layer is essentially on a straight line, and the movement and balance characteristics of the slanted upper, middle, and lower roofs are different. The maximum subsidence point of rock strata movement is located slightly above the middle of the inclination, which is also due to the support of the gangue filling, which is consistent with the results of the roof force analysis and deflection calculation in the normal mining stage in this paper.

(5) In the past, in mining the protective layer of near-horizontal and gently inclined coal seams, after the protective layer is mined, caving zones, fissure zones, and curved subsidence zones were usually formed above the goaf, referred to as "vertical three zones." From this experimental study, it can be found that the division of "vertical three belts" is not apparent. One of the reasons is that due to the large inclined angle (>45°) of the coal stratum, the force (inclination) component of the overlying strata along the roof layer is larger than the normal component along the layer, the vertical layer load is decomposed, and the roof collapse is not apparent. Another reason is that the thickness of the protective layer is small and the space for caving is limited, which is consistent with the conclusions obtained in the literature [36,37].

(6) From the similar experimental results, the mining activities of the lower protective layer caused the rock layer to move and extend to the top and bottom of the protected layer. The protected layer was within the protection range of the protective layer, and the coal seam conditions of the protected layer were not damaged. The fissures develop gradually from bottom to top with the expansion of the mining range until there are separation fissures in the roof of the protected layer. The development of abscission fissures dominates the whole experimental model, and small-scale interlayer fractures develop in local areas. Bedding and interlayer fractures intersect through the protective layer and the protected layer. The movement of rock formations and the development of fissures allow the protected layer to relieve pressure and provide an effective channel for extracting pressure-releasing gas.

## 5. Conclusions

(1) In the initial mining stage, before the roof collapses for the first time, there is no filling effect of the collapsed gangue, and the roof is in the elastic deformation stage. The deflection deformation is symmetrically distributed along the direction of the working face. The maximum deflection point along the working face is located slightly below the middle. In the normal mining stage, the maximum deflection point along the inclination of the working face is located slightly above the middle, which is less than the maximum deflection during the initial collapse. The reason why the maximum deflection position shifts upward along the slope is precisely due to the filling effect of the caving gangue.

(2) During the mining process of similar simulation experiments, the roof of the protective layer did not collapse on a large scale, and the roof was mainly sinking slowly. The maximum subsidence point of the overlying rock layers is essentially on a straight line, and the maximum subsidence point is slightly above the middle of the slope. The experimental results of the similar simulation are consistent with the roof force analysis results and deflection calculation in the normal mining stage.

(3) The steeply inclined coal seam has a large inclined angle of the coal seam so that the tangential component force along the rock layer increases. Furthermore, the vertical stress on the layer decreases, and the roof caving shape and pressure step distance differ from the coal seam with a slight inclination angle.

(4) Affected by the coal seam inclined angle and the mining layer's thickness, the "vertical three-zone" division of the goaf is not apparent. The mining of this type of lower

protective layer will not damage the mining conditions of the overlying protective layer. The development of fractures can provide a channel for the migration and extraction of pressure relief gas. The mining of this type of protective layer in this mine has good safety and feasibility.

**Author Contributions:** X.P.: Formal analysis and writing—original draft. L.Q.: Writing—review and editing. Z.W.: Methodology, project administration, supervision and validation, funding acquisition. X.Z.: Data processing and analysis. C.H.: Resources, data curation, and software. All authors have read and agreed to the published version of the manuscript.

**Funding:** This research was supported by the National Natural Science Foundation of China (Nos. 52074107 and 51704100); the Doctoral Fund of Henan Polytechnic University (No. B2016-004); the Postdoctoral Research Foundation of Henan Province.

**Institutional Review Board Statement:** Not applicable.

**Informed Consent Statement:** Not applicable.

**Data Availability Statement:** The original contributions presented in the study are included in the article, further inquiries can be directed to the corresponding author.

**Acknowledgments:** The authors would like to appreciate the editor and the reviewers for their useful and valuable comments and suggestions.

**Conflicts of Interest:** The authors declare no conflict of interest.

## References

1. Tu, H.; Tu, S.; Yuan, Y.; Wang, F.; Bai, Q. Present Situation of Fully Mechanized Mining Technology for Steeply Inclined Coal Seams in China. *Arab. J. Geosci.* **2015**, *8*, 4485–4494. [CrossRef]
2. Liu, H.; Liu, H.; Cheng, Y. The Elimination of Coal and Gas Outburst Disasters by Ultrathin Protective Seam Drilling Combined with Stress-Relief Gas Drainage in Xinggong Coalfield. *J. Nat. Gas Sci. Eng.* **2014**, *21*, 837–844. [CrossRef]
3. Peng, X.; Wang, Z.; Qi, L. Numerical Simulation of Gas-Solid Coupling in Pressure-Relief Gas Drainage of Short-Distance and Underprotective Steeply Inclined Coal Seam Mining. *Geofluids* **2022**, *2022*, 1979775. [CrossRef]
4. Cheng, X.; Zhao, G.; Li, Y.; Meng, X.; Tu, Q.; Huang, S.; Qin, Z. Mining-Induced Pressure-Relief Mechanism of Coal-Rock Mass for Different Protective Layer Mining Modes. *Adv. Mater. Sci. Eng.* **2021**, *2021*, 3598541. [CrossRef]
5. Niu, Y.; Wang, E.; Li, Z.; Gao, F.; Zhang, Z.; Li, B.; Zhang, X. Identification of Coal and Gas Outburst-Hazardous Zones by Electric Potential Inversion During Mining Process in Deep Coal Seam. *Rock Mech. Rock Eng.* **2022**, *55*, 3439–3450. [CrossRef]
6. Yang, W.; Lin, B.Q.; Qu, Y.A.; Zhao, S.; Zhai, C.; Jia, L.L.; Zhao, W.Q. Mechanism of Strata Deformation under Protective Seam and Its Application for Relieved Methane Control. *Int. J. Coal Geol.* **2011**, *85*, 300–306. [CrossRef]
7. Yin, G.; Li, M.; Wang, J.G.; Xu, J.; Li, W. Mechanical Behavior and Permeability Evolution of Gas Infiltrated Coals during Protective Layer Mining. *Int. J. Rock Mech. Min. Sci.* **2015**, *80*, 292–301. [CrossRef]
8. Chen, H.; Cheng, Y.; Ren, T.; Zhou, H.; Liu, Q. Permeability Distribution Characteristics of Protected Coal Seams during Unloading of the Coal Body. *Int. J. Rock Mech. Min. Sci.* **2014**, *71*, 105–116. [CrossRef]
9. Wang, H.; Cheng, Y.; Yuan, L. Gas Outburst Disasters and the Mining Technology of Key Protective Seam in Coal Seam Group in the Huainan Coalfield. *Nat. Hazards* **2013**, *67*, 763–782. [CrossRef]
10. Wang, L.; Lu, Z.; Chen, D.P.; Liu, Q.Q.; Chu, P.; Shu, L.Y.; Ullah, B.; Wen, Z.J. Safe Strategy for Coal and Gas Outburst Prevention in Deep-and-Thick Coal Seams Using a Soft Rock Protective Layer Mining. *Saf. Sci.* **2020**, *129*, 104800. [CrossRef]
11. Liu, H.; Cheng, Y. The Elimination of Coal and Gas Outburst Disasters by Long Distance Lower Protective Seam Mining Combined with Stress-Relief Gas Extraction in the Huaibei Coal Mine Area. *J. Nat. Gas Sci. Eng.* **2015**, *27*, 346–353. [CrossRef]
12. Liao, Z.; Feng, T.; Yu, W.; Wu, G.; Li, K. Experimental and Theoretical Investigation of Overburden Failure Law of Fully Mechanized Work Face in Steep Coal Seam. *Adv. Civ. Eng.* **2020**, *2020*, 8843172. [CrossRef]
13. Li, X.; Wang, Z.; Zhang, J. Stability of Roof Structure and Its Control in Steeply Inclined Coal Seams. *Int. J. Min. Sci. Technol.* **2017**, *27*, 359–364. [CrossRef]
14. Xie, P.; Wu, Y.; Wang, H.; Gao, X.; Zhang, Y.; Zeng, Y. Mechanism Analysis on Deformation and Failure of Gob-Side Entry in Soft Rock and Steep Coal Seam Group with Repeated Mining Operation. *Liaoning Gongcheng Jishu Daxue Xuebao (Ziran Kexue Ban)/J. Liaoning Tech. Univ. (Nat. Sci. Ed.)* **2013**, *32*, 44–49.
15. Zhang, J.W.; Wang, J.C.; Wei, W.J.; Chen, Y.; Song, Z.Y. Experimental and Numerical Investigation on Coal Drawing from Thick Steep Seam with Longwall Top Coal Caving Mining. *Arab. J. Geosci.* **2018**, *11*, 96. [CrossRef]
16. Wang, S.C.; Dou, L.M.; Mu, Z.L.; Cao, J.R.; Li, X.W. Study on Roof Breakage-Induced Roadway Coal Burst in an Extrathick Steeply Inclined Coal Seam. *Shock Vib.* **2019**, *2019*, 2969483. [CrossRef]

17. Hu, B.; Wu, Y.; Wang, H.; Tang, Y.; Wang, C. Risk Mitigation for Rockfall Hazards in Steeply Dipping Coal Seam: A Case Study in Xinjiang, Northwestern China. *Geomat. Nat. Hazards Risk* **2021**, *12*, 988–1014. [CrossRef]
18. Yuan, Z.; Shao, Y.; Zhu, Z. Similar Material Simulation Study on Protection Effect of Steeply Inclined Upper Protective Layer Mining with Varying Interlayer Distances. *Adv. Civ. Eng.* **2019**, *2019*, 9849635. [CrossRef]
19. Xie, P.; Wu, Y. Deformation and Failure Mechanisms and Support Structure Technologies for Goaf-Side Entries in Steep Multiple Seam Mining Disturbances. *Arch. Min. Sci.* **2019**, *64*, 561–574. [CrossRef]
20. Wu, Y.P.; Xie, P.S.; Wang, H.W.; Ren, S.G. Incline Masonry Structure around the Coal Face of Steeply Dipping Seam Mining. *Meitan Xuebao/J. China Coal Soc.* **2010**, *35*, 1252–1256.
21. Zeng, C.; Zhou, Y.; Zhang, L.; Mao, D.; Bai, K. Study on Overburden Failure Law and Surrounding Rock Deformation Control Technology of Mining through Fault. *PLoS ONE* **2022**, *17*, e0262243. [CrossRef] [PubMed]
22. Ning, J.; Wang, J.; Bu, T.; Hu, S.; Liu, X. An Innovative Support Structure for Gob-Side Entry Retention in Steep Coal Seam Mining. *Minerals* **2017**, *7*, 75. [CrossRef]
23. Liu, S.; Yang, K.; Tang, C.; Chi, X. Rupture and Migration Law of Disturbed Overburden during Slicing Mining of Steeply Dipping Thick Coal Seam. *Adv. Civ. Eng.* **2020**, *2020*, 8863547. [CrossRef]
24. Ventsel, E.; Krauthammer, T.; Carrera, E. Thin Plates and Shells: Theory, Analysis, and Applications. *Appl. Mech. Rev.* **2002**, *55*, B72–B73. [CrossRef]
25. Tu, H.; Tu, S.; Chen, F.; Wang, C.; Feng, Y. Study on the Deformation and Fracture Feature of Steep Inclined Coal Seam Roof Based on the Theory of Thin Plates. *J. Min. Saf. Eng.* **2014**, *31*, 49–54.
26. Li, X.; Chen, S.; Zhang, Q.; Gao, X.; Feng, F. Research on Theory, Simulation and Measurement of Stress Behavior under Regenerated Roof Condition. *Geomech. Eng.* **2021**, *26*, 49–61. [CrossRef]
27. Liu, H.; Zhang, B.; Li, X.; Liu, C.; Wang, C.; Wang, F.; Chen, D. Research on Roof Damage Mechanism and Control Technology of Gob-Side Entry Retaining under Close Distance Gob. *Eng. Fail. Anal.* **2022**, *138*, 106331. [CrossRef]
28. Zhang, B.; Cao, S. Study on First Caving Fracture Mechanism of Overlying Roof Rock in Steep Thick Coal Seam. *Int. J. Min. Sci. Technol.* **2015**, *25*, 133–138. [CrossRef]
29. Fan, X.G.; Wang, H.T.; Hu, G.Z.; Li, X.H.; Yuan, Z.G. Pressure-Relief Scope for the Exploiting of Steep-Inclined Oblique under-Protecting Strata. *Zhongguo Kuangye Daxue Xuebao/J. China Univ. Min. Technol.* **2010**, *39*, 380–385.
30. Wu, Y.; Yun, D.; Xie, P.; Wang, H.; Lang, D.; Hu, B. Progress, Practice and Scientific Issues in Steeply Dipping Coal Seams Fully-Mechanized Mining. *Meitan Xuebao/J. China Coal Soc.* **2020**, *45*, 24–34. [CrossRef]
31. Hongwei, W.; Yongping, W.; Jianqiang, J.; Peipei, C. Stability Mechanism and Control Technology for Fully Mechanized Caving Mining of Steeply Inclined Extra-Thick Seams with Variable Angles. *Min. Metall. Explor.* **2021**, *38*, 1047–1057. [CrossRef]
32. Chen, D.; Sun, C.; Wang, L. Collapse Behavior and Control of Hard Roofs in Steeply Inclined Coal Seams. *Bull. Eng. Geol. Environ.* **2021**, *80*, 1489–1505. [CrossRef]
33. Lu, P.; Zhang, P.Q.; Lee, H.P.; Wang, C.M.; Reddy, J.N. Non-Local Elastic Plate Theories. *Proc. R. Soc. A Math. Phys. Eng. Sci.* **2007**, *463*, 3225–3240. [CrossRef]
34. Wei, Z.; Yang, K.; Chi, X.; Liu, W.; Zhao, X. Dip Angle Effect on the Main Roof First Fracture and Instability in a Fully-Mechanized Workface of Steeply Dipping Coal Seams. *Shock Vib.* **2021**, *2021*, 5557107. [CrossRef]
35. Hong-Sheng, T.; Shi-Hao, T.; Cun, Z.; Lei, Z.; Xiao-Gang, Z. Characteristics of the Roof Behaviors and Mine Pressure Manifestations During the Mining of Steep Coal Seam. *Arch. Min. Sci.* **2017**, *62*, 871–891. [CrossRef]
36. Yin, G.; Dai, G.; Pi, W.; Zhang, D. Study on the Uneven Ground Pressure in Pitching Oblique Underhand Mining. *Yanshilixue Yu Gongcheng Xuebao/Chin. J. Rock Mech. Eng.* **2003**, *22*, 1483–1488.
37. Wu, Y.P.; Xie, P.S.; Ren, S.G. Analysis of Asymmetric Structure around Coal Face of Steeply Dipping Seam Mining. *Meitan Xuebao/J. China Coal Soc.* **2010**, *35*, 182–184.
38. Zhang, J.F.; Shi, P.W.; Zhang, H.M. Stability Analysis of Basic Roof after First Destruction in the Steep Seam. *Meitan Xuebao/J. China Coal Soc.* **2009**, *34*, 1160–1164.
39. Shi, F.; Wang, H.T.; Fan, X.G.; Yuan, Z.G.; Hu, G.Z. Mechanical Analysis of Main Roof Breakage with Dip Oblique Coal Mining Method. *Meitan Xuebao/J. China Coal Soc.* **2013**, *38*, 1001–1005.
40. Wu, Y.; Lang, D.; Xie, P.; Wang, H. Regional Fracture of Top-Coal along the Inclined Direction of Fully-Mechanized Caving Face in Soft Steep Dipping Seam. *Caikuang Yu Anquan Gongcheng Xuebao/J. Min. Saf. Eng.* **2018**, *35*, 553–560. [CrossRef]
41. Guo, Z.P.; Huang, W.P. Parameter Optimization and Stability Analysis of Inclined Gangue Strip-Fillings. *Meitan Xuebao/J. China Coal Soc.* **2011**, *36*, 234–238.
42. Tu, H.S.; Tu, S.H.; Zhu, D.F.; Hao, D.Y.; Miao, K.J. Force-Fracture Characteristics of the Roof above Goaf in a Steep Coal Seam: A Case Study of Xintie Coal Mine. *Geofluids* **2019**, *2019*, 7639159. [CrossRef]
43. Xie, P.S.; Wu, Y.P.; Wang, H.W.; Gao, X.C.; Ren, S.G.; Zeng, Y.F. Stability Analysis of Incline Masonry Structure and Support around Longwall Mining Face Area in Steeply Dipping Seam. *Meitan Xuebao/J. China Coal Soc.* **2012**, *37*, 1275–1280.